

The Updated Bottom Up Solution applied to mass spectrometry of soybean oil in a dietary supplement gelcap

William Craig Byrdwell

Received: 11 December 2014 / Revised: 11 February 2015 / Accepted: 23 February 2015 / Published online: 9 April 2015
© Springer-Verlag Berlin Heidelberg (outside the USA) 2015

Abstract Among the goals of lipidomics applied to triacylglycerols (TAGs) is identification of molecular species, degree and location of unsaturation, and positions of fatty acyl chains (i.e., identification of regioisomers). Toward those ends, we define one, two, and three “Critical Ratios” for Types I, II, and III TAGs that provided different aspects of the desired information. Critical Ratio 1, $[MH]^+/\Sigma[DAG]^+$, is correlated to the degree of unsaturation ($[MH]^+$ is the protonated molecule and $\Sigma[DAG]^+$ is the sum of diacylglycerol-like ions, $[DAG]^+$); Critical Ratio 2, $[AA]^+/[AB]^+$ for Type II TAGs (“ABA/AAB/BAA”) and $[AC]^+/([AB]^+ + [BC]^+)$ for Type III TAGs (“ABC/CBA/BAC/CAB/ACB/BCA”), is correlated to identification of regioisomers; and Critical Ratio 3, $[BC]^+/[AB]^+$, provides information about those $[DAG]^+$ from Type III TAGs. Furthermore, Critical Ratios are used in the Updated Bottom Up Solution (UBUS) to reproduce the mass spectra of TAGs by atmospheric pressure chemical ionization mass spectrometry applied to analysis of soybean oil in a dietary supplement gelcap. We present a new model for the $[MH]^+/\Sigma[DAG]^+$ ratio, quantify regioisomers using the $[AA]^+/[AB]^+$ ratio, and describe trends for $[BC]^+/[AB]^+$ that have never been reported before. The UBUS is also applied to other classes of molecules, i.e., vitamin D and DAGs. The amount of vita-

min D₃ in the gelcap fell from 2011 ± 22 when received to 1689 ± 33 just prior to expiration. The Critical Ratios constitute a compact data set that can provide structural information and also act as a library of mass spectra.

Keywords APCI-MS · Triacylglycerols · Regioisomers · Soybean oil · Lipidomics

Introduction

Triacylglycerols (TAGs) are important components of the human diet, and the fatty acids (FAs) (more precisely, fatty acyl chains) that make up TAGs have very different effects on human health, with saturated fats (SFAs), trans-FAs (TFAs), monounsaturated FAs (MUFAs), and polyunsaturated FAs (PUFAs) playing very different roles regarding cardiovascular health and other health outcomes. For instance, as Hunter [1] reviewed, unsaturated FAs tend to lower total cholesterol and low-density lipoprotein (LDL) concentrations, while saturated FAs (especially those $\leq 16:0$) tend to raise total cholesterol and LDL concentrations. A recent systematic review summarized the literature regarding effects of SFAs, MUFAs, and PUFAs on several health outcomes and serves as an excellent starting point for understanding the relationship between the types of FAs and cardiovascular disease (CVD), cancer, and type 2 diabetes [2]. The important point here is that the first two pieces of information about a fat or oil that are relevant to the diet and health are (1) the FA carbon chain length and (2) the degree of unsaturation.

In addition to the types of FAs in TAGs, the positions of the FAs on the TAG glycerol backbones play a significant role in their absorption and metabolism [1, 3–5]. The three positions that FAs can occupy on the glycerol backbone of a TAG are

Published in the topical collection *Lipidomics* with guest editor Michal Holčapek.

Electronic supplementary material The online version of this article (doi:10.1007/s00216-015-8590-9) contains supplementary material, which is available to authorized users.

W. C. Byrdwell (✉)

Food Composition and Methods Development Lab, Beltsville Human Nutrition Research Center, USDA, Agricultural Research Service, 10300 Baltimore Ave., Beltsville, MD 20705, USA
e-mail: C.Byrdwell@ars.usda.gov

referred to using the “stereospecific numbering” (*sn*) system, as positions *sn*-1, *sn*-2, and *sn*-3. TAGs having the same FAs, but arranged in different *sn* positions, are referred to as regioisomers. The identities of regioisomers are important because lipases in the human body show regioselectivity in the degradation of TAGs. As discussed in the review by Mu and Porsgaard [4], lingual and gastric lipases are regioselective for FAs in the *sn*-3 position, while pancreatic lipase, which is responsible for the bulk of TAG metabolism into 2-monoacylglycerols (2-MAGs) and free FAs (FFAs), performs hydrolysis at the *sn*-1 and *sn*-3 positions. Thus, the FA that is in the *sn*-2 position tends to be conserved. Some rearrangement of the 2-MAGs does occur, however, meaning that conservation of the FA in the *sn*-2 position is not absolute. The efficiency of enzymatic hydrolysis of the *sn*-1 and *sn*-3 positions, as well as the likelihood of FA migration in the 2-MAG, also depends on the length and degree of unsaturation of the FAs at those positions [4].

Not only is there regioselectivity in the way fats are metabolized in the human body but also in the formation of fats in plants and animals [1, 5, 6]. Therefore, there is an obvious need for tools to assess not only the carbon chain length and degree of unsaturation of FAs in TAGs but also the locations of those FAs on the TAG backbones.

The two most popular forms of LC-MS for TAG analysis use the atmospheric pressure ionization (API) techniques of atmospheric pressure chemical ionization (APCI) [7–11] and electrospray ionization (ESI) [12–17], which these applications have been previously reviewed for APCI-MS [18–20] and ESI-MS [21–25]. Mottram and Evershed [26] first constructed and reported the $[AA]^+/[AB]^+$ for TAGs for identification of regioisomers using APCI-MS. Although Fauconnot et al. [27] tabulated values for $[AA]^+/[AB]^+$ for some TAG, they performed quantification of regioisomers using what they called the “regioisomeric purity” ratio, although Byrdwell showed that this ratio could be simplified [28]. Others have simply expressed raw relative abundances [29]. We have found that the ratio originally expressed by Mottram and Evershed [26] and used later by Jakab et al. [30] represents a very efficient, effective means of conveying the desired information. By analogy to this ratio used for Type II TAG, Byrdwell constructed the $[AC]^+/([AB]^+ + [BC]^+)$ ratio to derive the analogous information about regioisomers of Type III TAGs [28].

A different ratio was constructed by Byrdwell [28] to reflect the other primary trend, which relates the degree of unsaturation to the relative proportion of the $[MH]^+$ ion versus the $[DAG]^+$ ions (i.e., unsaturated TAGs give a higher $[MH]^+$ and lower $[DAG]^+$, while less or no unsaturation produces lower $[MH]^+$ and higher $[DAG]^+$ abundances). The ratio used to reflect this relationship was the $[MH]^+/\Sigma[DAG]^+$ ratio. Taken together, Byrdwell [28] referred to these ratios ($[AA]^+/[AB]^+$, $[AC]^+/([AB]^+ + [BC]^+)$ and $[MH]^+/\Sigma[DAG]^+$)

as “Critical Ratios” since these are the simplest ratios that express the critical structural information about the unsaturation and regioisomer identities of TAGs. For type III TAGs, one other Critical Ratio was specified, which is the $[BC]^+/[AB]^+$ ratio.

Since APCI is not able to differentiate the *sn*-1 and *sn*-3 positions, and no trends for $[sn-1,2-AB]^+$ versus $[sn-2,3-BC]^+$ had been previously reported, Byrdwell proposed [28]: “In the absence of a definitive trend, the data can be used to try to elucidate any subtle trends that may not be readily apparent. If one chooses to set the $[BC]^+$ fragment equal to the smaller of the two possible abundances for $[AB]^+$ or $[BC]^+$, then perhaps the ratios will indicate some structural trends.”

Before proceeding, one other trend should be mentioned. Laakso and Voutilainen [10] and Manninen and Laakso [31] first reported that the distances of the double bonds from the methyl ends of the acyl chains in TAGs also affected the $[DAG]^+$ fragment abundances. They showed that when the unsaturation is further from the terminal methyl (i.e., *n*-6 Ln), which is closer to the carbonyl moiety, the acyl moiety fragment was more stable, was more easily lost, and resulted in higher proportions of the fragment formed by loss of that moiety. Thus, for *n*-6 OLnO, the $[AA]^+/[AB]^+$ ratio was much higher than for *n*-3 OLnO because the *n*-6 Ln was more easily lost and produced a larger $[AA]^+$ fragment.

Reported here are the clarification, simplification, and expansion of the Bottom Up Solution that was previously reported. It is clarified to provide additional explanation and understanding of the BUS. It is simplified to show that the value of unity (1) and the Critical Values used earlier are important and useful to help understand the BUS construct, but classification into the Cases can be accomplished using only the Critical Limits (the Critical Values, Critical Limits, and Cases were described previously [28] and are further explained below). The BUS is also simplified by taking advantage of similarities to streamline the Case classifications. Finally, the BUS is expanded by using the Critical Ratios to characterize structural trends in greater detail than previously allowed. Since minor improvements have been made to the BUS for clarity and simplification, the updated version of the construct is referred to as the Updated Bottom Up Solution (UBUS) to differentiate it from the original BUS, although the BUS remains perfectly valid.

Materials and methods

Chemicals and supplies

The following solvents were Optima LC-MS grade or the highest grade available and were purchased from Thermo Fisher Scientific, Inc. (Fairlawn, NJ, USA): acetonitrile (ACN), methylene chloride (dichloromethane, DCM), and

methanol (MeOH). Ammonium formate was from Sigma-Aldrich, Inc. (St. Louis, MO, USA). Samples were 2000 international units (IU, where 1 IU=0.025 µg) vitamin D₃ supplements in soybean oil and were purchased from an online herbal supplement supplier, which were kept refrigerated until analysis. Samples and vitamin D₃ calibration standards were prepared according to the “dilute-and-shoot” protocol described previously [32].

Liquid chromatography

The Agilent 1200 LC system from Agilent Technologies, Inc. (Santa Clara, CA, USA) has been recently described [33]. After the outlet of the UV DAD, the effluent went to a series of Valco tees (Valco Instruments, Inc., Houston, TX, USA) with fused silica tubing, specific lengths, diameters, and resultant flow rates of which have been reported previously [33].

Data from a corona-charged aerosol detector (CAD) ultra RS (Thermo Scientific Dionex, Sunnyvale, CA, USA) and 1290 Infinity (#G4261B) evaporative light scattering detector (ELSD) (Agilent Technologies, Inc., Santa Clara, CA, USA) were acquired, but are not discussed herein. UV data were acquired for analysis of vitamin D₃ in the dietary supplement since we have repeatedly shown that, as long as MS is used to verify the purity of the peaks, UV data provides quantification with lower %RSD than MS.

Mass spectrometry

Four mass spectrometers were used simultaneously in parallel for this analysis, a high-sensitivity APCI-MS instrument, i.e., a TSQ Vantage EMR (Thermo Scientific, Inc., San Jose, CA, USA), a low-sensitivity APCI-MS instrument, i.e., a TSQ 7000 (Thermo Scientific, Inc.), ESI-MS on an LCQ Deca XP (Thermo Scientific, Inc.), and APPI-MS on an AB Sciex QTrap 4000 mass spectrometer. Specific source and scan parameters for APCI-MS and ESI-MS have been provided in detail recently [32], while APPI-MS used the same source parameters as ESI-MS on the QTrap 4000 [33]. Quantification was performed only on the newer, more sensitive APCI-MS instrument since only one set of APCI-MS data is needed to demonstrate the principles associated with structural analysis of TAGs by APCI-MS.

The average mass spectrum across every integrated peak for every replicate from each of the three mass spectrometers used for quantification was obtained and pasted into a Microsoft Excel spreadsheet, and these were used to calculate the Critical Ratios.

For TAG quantification, the method of Byrdwell et al. [9] was used in which the TAGs were analyzed by LC-MS and the fatty acid methyl esters (FAME) from the TAGs were analyzed by gas chromatography (GC) with flame ionization

detection (FID). This approach compares the molar FA composition calculated from the FAME composition to the FA composition calculated from the TAG composition determined by LC-MS to produce response factors for each FA, which are then used to produce TAG response factors. This has been explained in greater detail elsewhere [21, 34]. A workbook of Microsoft Excel spreadsheets to calculate response factors is provided in the Electronic Supplementary Material (ESM).

Also, the recent innovation implemented by Byrdwell [33, 35] was applied in which the $1x^{13}C$ isotopic peaks were included with the monoisotopic peaks for quantification to increase the signal usable by ~30 to 60 % (depending on whether it is a $[DAG]^+$ or $[MH]^+$). Furthermore, all ions for the $[MH]^+$ and $[DAG]^+$ corresponding to each TAG were extracted together in group-extracted ion chromatograms (EICs) instead of separate EICs for each m/z . This had advantages of increasing the total signal for each TAG, allowing TAGs at low levels to be quantified with more confidence and of decreasing the number of EICs that required integration. The one disadvantage of this procedure is that when two TAGs share the same or isobaric $[DAG]^+$ fragments (e.g., $[OLn]^+=[LL]^+$ at m/z 599.6 from $OLnL$ and LLL), there is not the option to apportion the integrated area between two TAGs, as we have done in the past [36].

FA abbreviations

The following abbreviations were used for identification of fatty acids and fatty acyl chains in TAGs and DAGs given as carbon chain length:sites of unsaturation: Cy: caprylic, C8:0; Ca: capric, C10:0; M: myristic, C14:0; P: palmitic, C16:0; Po: palmitoleic, 16:1; S: stearic, C18:0; O: oleic, C18:1; L: linoleic, 18:2; Ln: linolenic, C18:3; A: arachidic, C20:0; G: gadoleic, C20:1; B: behenic, C22:0; E: erucic, C22:1; Lg: lignoceric, C24:0; N: nervonic, C24:1; Ce: cerotic, C26:0; Mo: montanic, C28:0.

Results

Table 1 shows a summary of results for the soybean oil TAGs and other triacylglycerols in the gelcap. APCI-MS showed excellent agreement to the FA composition by GC-FID given in Table 2. The three TAGs containing “Cy” and “Ca” fatty acyl chains were quantified separately from the other TAGs because they did not originate from the soybean oil. These three TAGs constituted 0.90 ± 0.04 % of RF-adjusted TAG area abundances by APCI-MS. We previously showed [32] that a different brand of gelcap that also used vitamin D₃ from fish oil similarly contained these same three short-chain TAGs.

Table 1 Response factor-adjusted percentage composition and isotope-adjusted Critical Ratios for soybean oil from vitamin D₃-containing supplement gelcap determined by APCI-MS on the TSQ Vantage EMR mass spectrometer

TAG	RT	% Comp.	[MH] ⁺ /Σ[DAG] ⁺	[AA] ⁺ /[AB] ⁺	Case	
CyCyCy	12.67	24.12	0.0170		1	
CyCyCa	16.56	46.57	0.0161	0.4856	1.1	
CaCaCy	22.11	29.31	0.0103	0.5620	1.1	
TAG	RT	% Comp	[MH] ⁺ /Σ[DAG] ⁺	[AA] ⁺ /[AB] ⁺ or [AC] ⁺ /([AB] ⁺ + [BC] ⁺)	[BC] ⁺ /[AB] ⁺	Case
LnLnLn	46.71	0.09	4.6048			2
LnLLn	49.49	1.25	4.5895	0.4876		2.1
LLnL	52.82	6.89	3.9516	0.4684		2.1
LnOLn	53.57	0.47	5.1956	0.5725		2.1
<i>LnLM</i>	55.03	0.08	1.6578	0.1468	0.3161	2.1.1
LnLnP	55.40	0.26	3.2613	1.3306		2.2
LLL	56.83	14.32	2.6639			2
LLnO	57.78	4.35	2.4396	0.4244	0.8439	2.1.1
<i>LLM</i>	59.55	0.29	1.5774	1.5468		2.2
LnLP	59.92	3.44	2.2242	0.2598	0.5431	2.1.1
<i>LnPPo</i>	60.48	0.08	0.6776	0.2016	0.4171	2.1.1
<i>LnOM</i>	60.55	0.09	1.1015	0.1790	0.8210	2.1.1
LLO	62.64	13.62	1.3802	0.8761		2.1
<i>OLPo</i>	63.76	0.21	0.4566	0.1994	0.5142	1.1.1
<i>OLnO</i>	63.77	1.23	1.5315	0.4271		2.1
LLP	65.18	11.71	1.2704	1.3171		2.2
<i>LOM</i>	66.21	0.31	0.4981	0.2626	0.6711	2.1.1
<i>PoLP</i>	66.30	0.43	0.2102	0.1568	0.2950	1.1.1
OLnP	66.36	1.11	1.0793	0.3528	0.5498	2.1.1
LLG	67.85	0.41	1.3672	1.9664		2.2
<i>PLM</i>	69.07	0.12	0.0401	0.3335	0.9483	1.1.1
<i>PLnP</i>	69.28	0.17	0.3373	0.2869		1.1
OLO	69.62	6.75	0.6720	0.2550		1.1
<i>MOM</i>	70.46	0.07	0.0824	0.2658		1.1
<i>OOPo</i>	71.42	0.43	0.0784	5.6475		1.2
LLS	71.55	4.44	1.3880	1.1269		2.2
<i>LLnA</i>	71.68	0.09	1.6129	0.3007	0.8362	2.1.1
OLP^a	72.73	7.65	0.3282	0.3410	0.4968	1.1.1
<i>SLnO</i>	72.98	0.74	0.1556	0.0549	0.0832	1.1.1
<i>OOM</i>	74.10	0.23	0.2157	0.4667		1.1
<i>PoPO</i>	74.17	0.23	0.1307	0.3968	0.7211	1.1.1
<i>OLG</i>	75.55	0.36	0.5574	0.0904	0.6505	2.1.1
PLP	76.10	2.32	0.0332	0.3787		1.1
<i>POM</i>	77.75	0.16	0.0583	0.2489	0.9287	1.1.1
OOO	77.83	2.64	0.2370			1
<i>LLnB^a</i>	78.29	0.11	1.9373	0.4337	0.8350	2.1.1
<i>LLA</i>	78.42	0.27	1.4520	1.2353		2.2
<i>LGP</i>	79.13	0.22	1.0087	0.3499	0.5888	2.1.1
LOS^a	79.97	2.97	0.3525	0.3119	0.5019	1.1.1
OOP	81.52	2.34	0.1224	0.6005		1.1
<i>LL-21:0</i>	81.94	0.06	1.2333	1.7099		2.2
<i>OLE</i>	82.74	0.05	0.5942	0.2913	0.6940	2.1.1
SLP	83.82	1.66	0.0320	0.3757	0.8630	1.1.1

Table 1 (continued)

TAG	RT	% Comp	[MH] ⁺ /Σ[DAG] ⁺	[AA] ⁺ /[AB] ⁺ or [AC] ⁺ /([AB] ⁺ + [BC] ⁺)	[BC] ⁺ /[AB] ⁺	Case
<i>OOG</i>	84.24	0.31	0.1624	1.5728		1.2
<i>LnLLg</i>	85.46	0.03	1.9964	0.3691	0.7453	2.1.1
POP	85.62	0.68	0.0579	0.2650		1.1
<i>LLB</i>	85.70	0.32	1.4945	1.1261		2.2
<i>OLA</i>	87.68	0.16	0.3333	0.3520	0.7440	1.1.1
<i>PGO</i>	88.73	0.16	0.1931	0.3621	0.7107	1.1.1
<i>LL-23:0</i>	89.52	0.07	1.5755	1.2788		2.2
OOS	89.66	0.88	0.1244	0.5101		1.1
<i>OL-21:0^a</i>	91.67	0.03	0.3111	0.2702	0.3719	1.1.1
<i>PPP</i>	91.77	0.01	0.0027			1
<i>PAL</i>	91.99	0.21	0.0654	0.2339	0.5330	1.1.1
SLS	92.07	0.39	0.0406	0.5066		1.1
<i>OOE</i>	92.22	0.13	0.1005	3.7514		1.2
LLLg	93.30	0.10	1.5179	0.9437		2.1
SOP	94.13	0.51	0.0619	0.1392	0.8773	1.1.1
OLB^a	95.52	0.18	0.3445	0.3838	0.7007	1.1.1
EPO	96.78	0.04	0.2158	0.4388	0.8378	1.1.1
<i>GSO</i>	96.83	0.05	0.2858	0.2912	0.5240	1.1.1
<i>LL-25:0</i>	97.13	0.02	1.3931	1.3114		2.2
OOA	97.77	0.06	0.1501	0.5128		1.1
<i>LO-23:0</i>	99.51	0.03	0.3335	0.3292	0.5363	1.1.1
LBP	99.96	0.15	0.0401	0.3336	0.9683	1.1.1
<i>SAL</i>	100.20	0.08	0.0541	0.3094	0.5424	1.1.1
<i>PPS</i>	101.01	0.01	0.0017	0.6582		1.1
<i>LLCe</i>	101.02	0.02	1.4493	1.2031		2.2
<i>OO-21:0</i>	101.83	0.01	0.1106	1.0218		1.2
<i>AOP^a</i>	102.73	0.06	0.1589	0.4492	0.8384	1.1.1
SOS	102.86	0.13	0.0841	0.1990		1.1
<i>OLLg^a</i>	103.45	0.07	0.3278	0.3967	0.7968	1.1.1
OOB	105.84	0.08	0.1510	0.4703		1.1
<i>LO-25:0</i>	107.17	0.01	0.3110	0.3026	0.4531	1.1.1
<i>PLgL</i>	107.70	0.06	0.0546	0.2671	0.5833	1.1.1
SBL	108.17	0.06	0.0446	0.3191	0.8497	1.1.1
<i>OO-23</i>	109.30	0.01	0.1085	0.7239		1.1
BOP^a	110.08	0.04	0.0707	0.4155	0.7780	1.1.1
<i>OLCe</i>	110.25	0.01	0.3330	0.3100	0.6618	1.1.1
<i>SAO</i>	110.40	0.02	0.1099	0.3342	0.6492	1.1.1
OOLg	112.50	0.03	0.1324	0.4555		1.1
SLgL	114.37	0.01	0.0375	0.4625	0.9766	1.1.1
OO-25	115.14	0.00	0.0927	0.9054		1.1
OLgP	115.86	0.01	0.0692	0.4248	0.7213	1.1.1
BOS	116.37	0.01	0.0632	0.3628	0.8016	1.1.1
OOCe	117.39	0.01	0.1376	0.5022		1.1
LSCe	118.47	0.00	0.0338	0.3640	0.7702	1.1.1
LgOS	119.28	0.01	0.0620	0.4853	0.7035	1.1.1
<i>OOMo</i>	119.57	0.00	0.1383	1.9521		1.2
Sum		100.00				

TAG name indicates most abundant regioisomer, as indicated by Critical Ratio 2, and order of fatty acyl chains indicated by Critical Ratio 3 set to less than 1. Bold indicates clean spectrum. Italics indicate spectrum contains substantial peaks from more than one TAG

^a Order of FA changed after isotope correction

$[\text{MH}]^+/\Sigma[\text{DAG}]^+$ ratio models

Figure 1 shows the $[\text{MH}]^+/\Sigma[\text{DAG}]^+$ ratios of soybean oil TAGs (as blue diamonds) plotted versus the degree of unsaturation. The calculated $[\text{MH}]^+/\Sigma[\text{DAG}]^+$ values from the 1/3 power fit are plotted as red squares in Fig. 1 obtained from the equation adapted and updated from Ref. [36].

Critical Ratio 1 in Fig. 1 appears to show a sigmoid (s-shaped curve) distribution, so a sigmoid model was also plotted based on the standard natural logarithmic sigmoid equation $f(x)=1/(1+e^{-x})$ (http://en.wikipedia.org/wiki/Sigmoid_function). The sigmoid function not only used the same inflection point and value for LnLnLn as the 1/3 power fit but also included a scaling factor to give the following:

$$\text{Sigmoid TAG function} = C_1 \times S \times \left(\frac{1}{1 + e^{C_2 - \text{sites}}} \right) \quad (1)$$

where the first constant C_1 =the $[\text{MH}]^+/\Sigma[\text{DAG}]^+$ obtained from LnLnLn (=4.6048; Table 1); “sites” is the number of

Table 2 Mole percentage fatty acid (FA) compositions from the FA methyl esters (FAME) by GC with a flame ionization detector (FID) and calculated from the response factor-adjusted triacylglycerol (TAG) compositions determined by atmospheric pressure chemical ionization (APCI) mass spectrometry (MS)

FA	GC-FID (%)	APCI-MS (%)
Cy ^a	64.41	66.89
Ca	35.59	33.11
Sum	100.00	100.00
M	0.48	0.47
Po	0.51	0.46
P	12.17	12.33
Ln	7.62	7.60
L	50.47	51.10
O	23.22	22.49
S	4.11	4.15
A	0.31	0.32
G	0.52	0.50
21	0.03	0.03
B	0.31	0.31
E	0.04	0.07
23	0.03	0.04
Lg	0.11	0.11
N	0.03	0.00
25	0.01	0.01
Ce	0.01	0.01
Mo	0.00	0.00
Sum	100.00	100.00
%DAG/TAG		0.90

^a Short-chain TAGs came only from samples using vitamin D₃ from fish oil

sites of unsaturation, from 0 to 9; the second constant, $C_2=5.5$, was selected as the inflection point of the function; and S is a scaling factor set to $S=1.03$. Figure 1 shows that the sigmoid TAG function gave values (green triangles in Fig. 1) closer to the average values (purple circles in Fig. 1) than the 1/3 power fit, so it represents a better model of Critical Ratio 1. The information and knowledge that correlate the Critical Ratios with structural characteristics of TAGs are referred to as the Interpretation Matrix for the BUS and the UBUS.

In Table 1 and Fig. 1, only two TAGs have seven sites of unsaturation, LLLn and LnLnO, and these two are isobaric, so they have the exact same $[\text{MH}]^+$ mass. Since LnLnO eluted on the tail of the much larger LLLn peak (0.47 versus 6.89 %), the $[\text{MH}]^+$ from the larger amount of LLLn caused the $[\text{MH}]^+/\Sigma[\text{DAG}]^+$ ratio for LnLnO to be higher, so the average shown in Fig. 1 was calculated with and without the higher value for comparison.

Critical Ratio 1: $[\text{MH}]^+/\Sigma[\text{DAG}]^+$

In the BUS [28], if the TAGs showed a $[\text{MH}]^+$ base peak, the $[\text{MH}]^+/\Sigma[\text{DAG}]^+$ Critical Ratio was classified as case 2, whereas if TAG had fewer sites of unsaturation, a $[\text{DAG}]^+$ was the base peak, and the $[\text{MH}]^+/\Sigma[\text{DAG}]^+$ was classified as Case 1. Thus, just the Case classification alone indicated whether the $[\text{MH}]^+$ or the $[\text{DAG}]^+$ was the base peak for all TAG Types (I, II, and III).

In the UBUS, the schemes are relabeled Scheme I, Scheme II, and Scheme IIIA, B to correspond to Types I, II, and III TAGs, respectively, instead of being part I, part II,

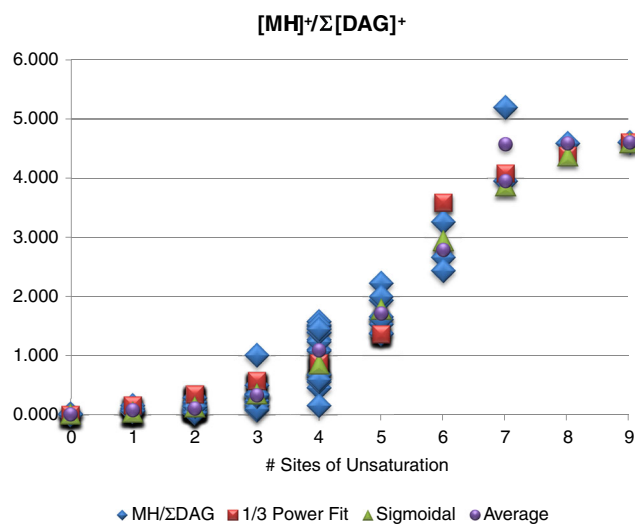
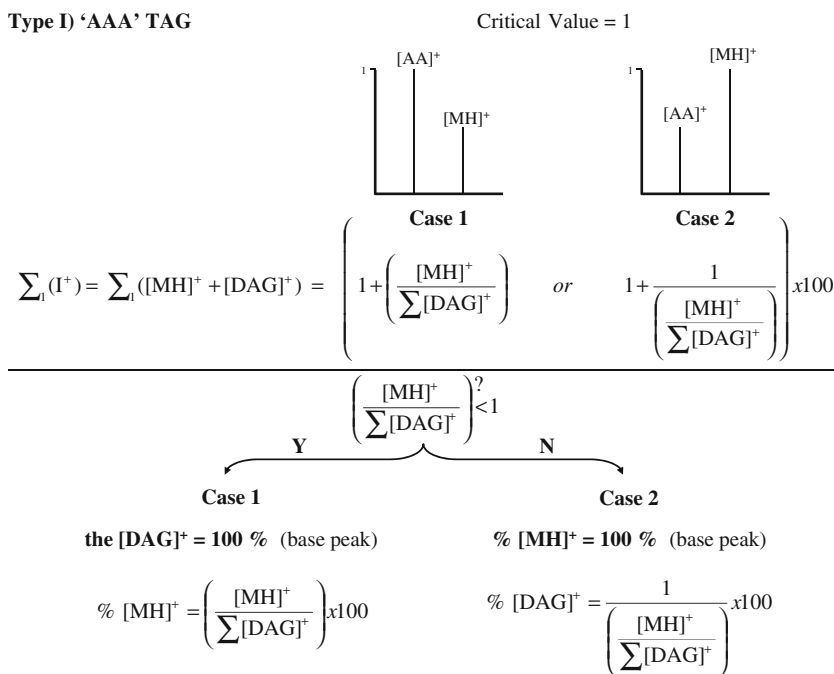


Fig. 1 Plot of $[\text{MH}]^+/\Sigma[\text{DAG}]^+$ ratios and averages from APCI-MS data for soybean oil triacylglycerols (see Table 1) and model ratios from “1/3 power fit” [36] and sigmoidal fit for 0 to 9 sites of unsaturation. Minimum value=0, maximum value set to the $[\text{MH}]^+/\Sigma[\text{DAG}]^+$ ratio for LnLnLn (=4.6048), and inflection point set to 5.5 for both model functions. The average for the seven sites is shown with (upper) and without (lower) LnLnO (0.47 % comp.) due to interference from LLLn

Scheme I Equations to calculate the relative abundances of the $[MH]^+$ ion and the $[DAG]^+$ fragment ion for a Type I TAG using the $[MH]^+/\Sigma[DAG]^+$ Critical Ratio in Table 1

Type I) 'AAA' TAG



and part III of Scheme I. Another change was based on the fact that the logical test for case classification could be expressed either as “if $[MH]^+/\Sigma[DAG]^+ \leq 1$, then Case 1, else Case 2” or as “if $[MH]^+/\Sigma[DAG]^+ \geq 1$, then Case 2, else Case 1.” For simplicity and uniformity, the UBUS logical tests have been chosen as “if $[MH]^+/\Sigma[DAG]^+ < 1$, then Case 1, else Case 2.”

Critical Values

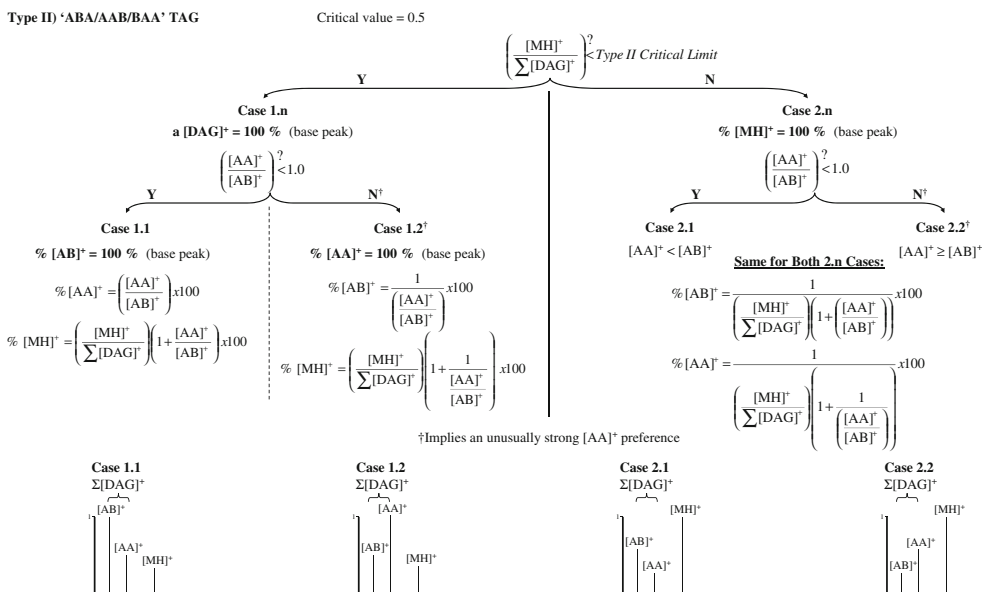
For Types I, II, and III TAGs, there is a value inherent in the construction of the $[MH]^+/\Sigma[DAG]^+$ ratio such that if the first Critical Ratio is less than that value, it is mathematically

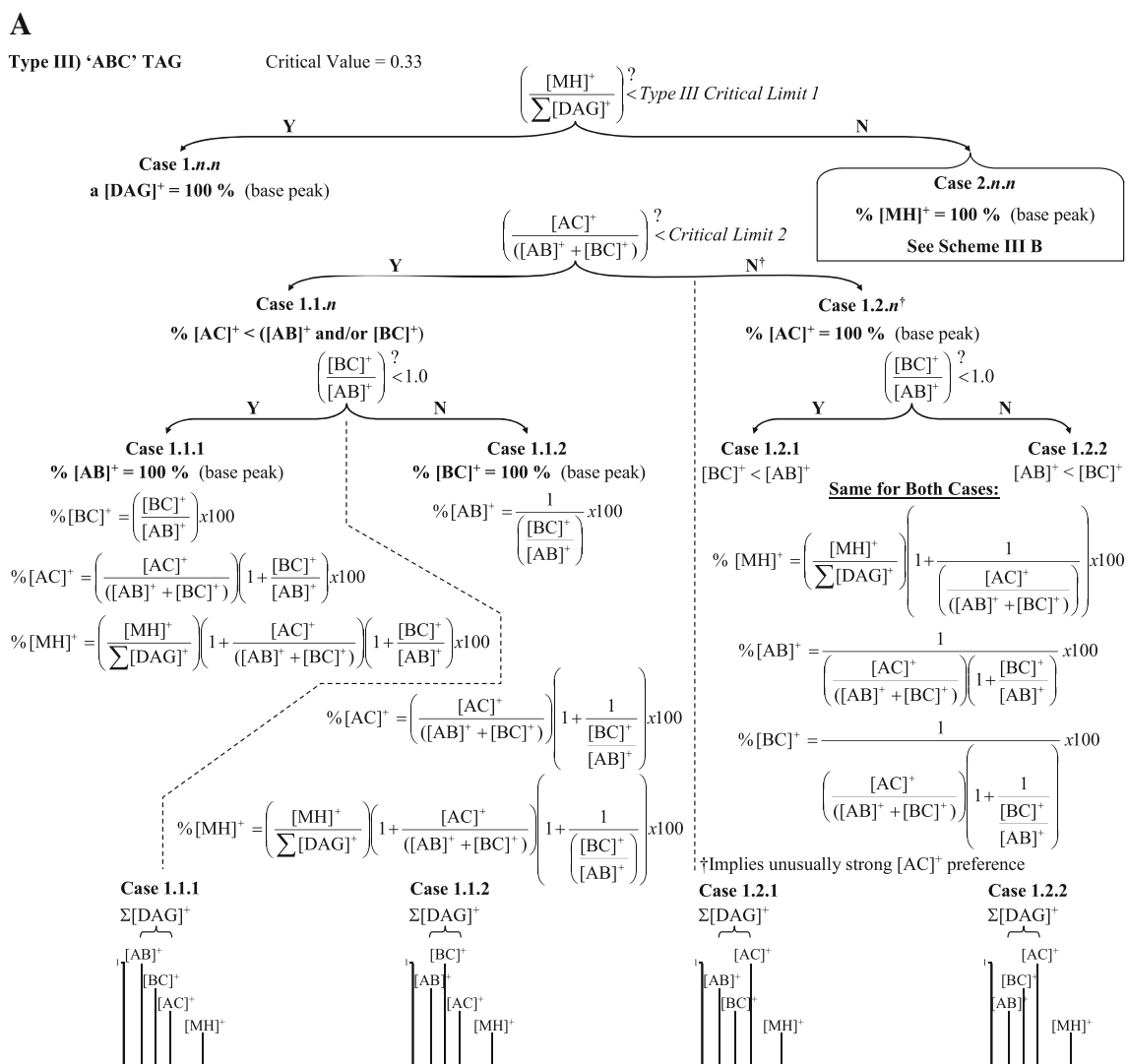
impossible for the TAG to have an $[MH]^+$ base peak. This value for each type of TAG is called the Critical Value and is determined by setting all abundances to their maximum values of 100 %, as shown in Fig. 2. This is highly unlikely in real mass spectra, but serves as a mathematical limiting case.

A second mathematical limiting case is inherent in Critical Ratio 1. If the $[MH]^+/\Sigma[DAG]^+$ ratio is greater than 1, then the TAG must have a Case 2 mass spectrum, which has an $[MH]^+$ base peak for any Types I, II, or III TAG. Thus, Critical Values form the lower boundary for the $[MH]^+/\Sigma[DAG]^+$ ratio, below which the $[MH]^+$ cannot be the base peak, and 1 serves as

Scheme II Equations to calculate the relative abundances of the $[MH]^+$ ion and $[DAG]^+$ fragment ions for Type II TAGs using two Critical Ratios from APCI-MS data (Table 1), $[MH]^+/\Sigma[DAG]^+$ and $[AA]^+/[AB]^+$. The Critical Limit for a Type II TAG is given in Fig. 3

Type II) 'ABA/AAB/BAA' TAG





Scheme III A Case 1 equations to calculate the relative abundances of the $[\text{MH}]^+$ and $[\text{DAG}]^+$ fragment ions for Type III TAGs (= "ABC"), Case 1.n.n, using Critical Ratios from APCI-MS data (Table 1). Critical Limit 1 and Critical Limit 2 for Type III TAGs are given in Fig. 3

the upper boundary, above which the $[\text{MH}]^+$ must be the base peak.

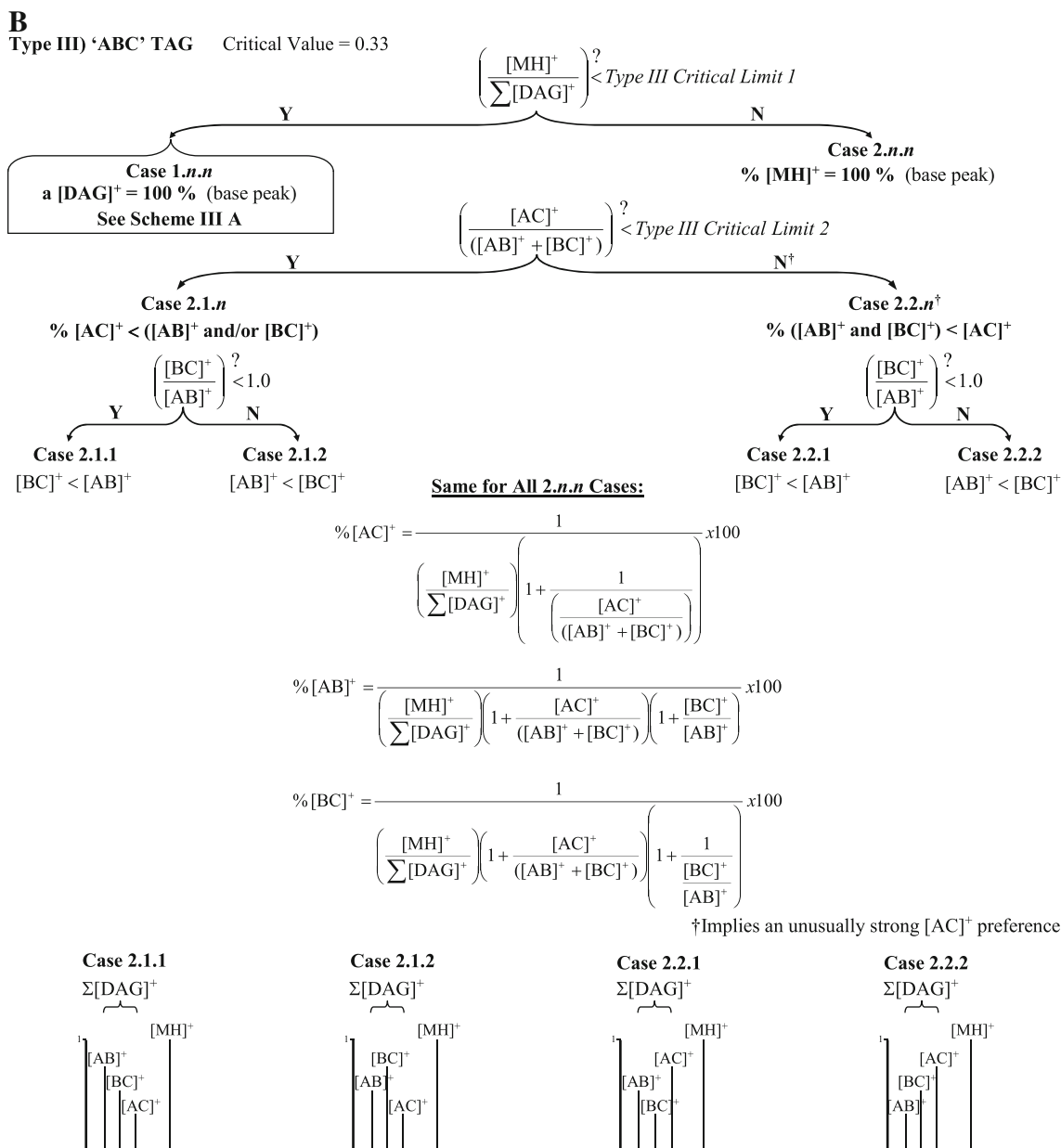
While those boundary conditions were important to understand the BUS construct, as a pragmatic matter, the Case classification for the $[\text{MH}]^+/\sum[\text{DAG}]^+$ ratio can be accomplished by using only the Critical Limits (described previously [28] and below). Therefore, to simplify the UBUS, the only Case classification criteria that are shown for the $[\text{MH}]^+/\sum[\text{DAG}]^+$ ratio in the schemes are based on the Critical Limits.

Critical Limits

While Critical Values were based on the boundary condition where all $[\text{MH}]^+$ and $[\text{DAG}]^+$ abundances being 100 %, Critical Limits, depicted in Fig. 3, are based on the limiting condition where two abundances are 100 %, and if either one

were to decrease by the least amount, the other one would be the base peak. The Critical Limits are based on the real Critical Ratios observed with only two abundances idealized (100 %), instead of the completely idealized theoretical spectra used to determine the Critical Values.

Before discussing the Case classification based on Critical Limits further, another simplification to the BUS will be mentioned. In the BUS, Cases 1, 3, and 5 were all examples of the Critical Ratios less than 1 or the Critical Limit, while Cases 2, 4, and 6 were all examples of the Critical Ratios greater than 1 or the Critical Limit. Thus, a Case 1.3.5 TAG can be called more simply a 1.1.1 TAG, a Case 2.4.6 TAG can be referred to as a Case 2.2.2 TAG, and every combination between. Thus, all possible classifications are as follows (see Schemes): Type I: Case 1, Case 2; Type II: Case 1.1, Case 1.2, Case 2.1, Case 2.2; and Type III: Case 1.1.1, Case 1.1.2, Case 1.2.1, Case 1.2.2, Case 2.1.1, Case 2.1.2, Case 2.2.1, and Case 2.2.2.



Scheme III B Case 2 equations to calculate the relative abundances of the $[\text{MH}]^+$ and $[\text{DAG}]^+$ fragment ions for Type III TAG (= "ABC"), Case 2.n.n, using Critical Ratios from APCI-MS data (Table 1). Critical Limit 1 and Critical Limit 2 for Type III TAGs are given in Fig. 3

Critical Ratio 2 for Type II TAGs: $[\text{AA}]^+ / [\text{AB}]^+$

If there were no discrimination or preference for formation of particular $[\text{DAG}]^+$ fragments, they would have the same abundances, and $[\text{AA}]^+ / [\text{AB}]^+ (= [\text{AA}]^+ / ([\text{AB}]^+ + [\text{BA}]^+))$ or $[\text{AC}]^+ / ([\text{AB}]^+ + [\text{BC}]^+)$ would always be 1/2 or 0.5. However, since loss of the FA in the *sn*-2 position is energetically disfavored, Critical Ratio 2 can be used to assign the FA in the *sn*-2 position. The names of the TAGs in the tables herein are written to reflect this fact. This information represents another important aspect of the Interpretation Matrix that relates $[\text{DAG}]^+$ abundances to TAG structures.

Note that for Type II TAGs, the conventional nomenclature ABA/AAB/BAA has a somewhat different meaning than for Type III TAGs, ABC/CBA/BAC/CAB/ACB/BCA. For Type II TAGs, the "A" represents the specific FA that there are two of, while the "B" represents the FA that there is only one of, regardless of their positions on the glycerol backbone. For Type III TAGs, the "A," "B," and "C" could represent any of the FAs, unless otherwise specified. Usually, the specific FAs in Type III TAGS are assigned based on the regioisomers identified by MS, with the fragment having the lowest abundance being assigned as the $[\text{AC}]^+$ fragment. This convention is followed in Table 1 and **ESM** Tables. For Type II TAGs, the

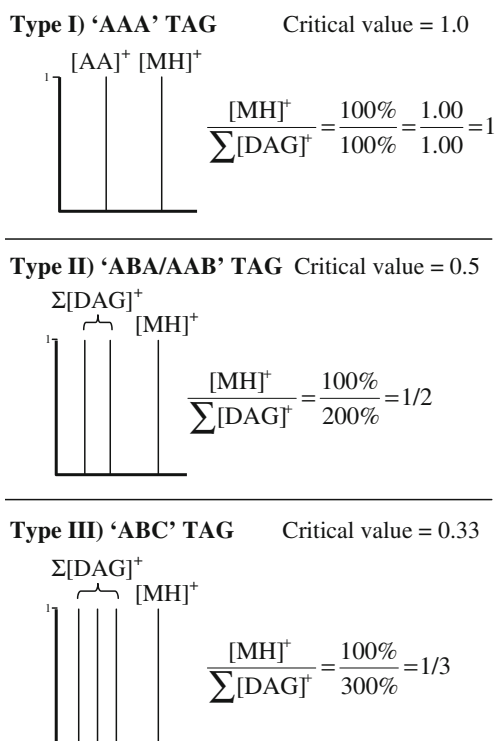


Fig. 2 Generalized representations of mass spectra used to calculate Critical Values for the $[MH]^+/\sum[DAG]^+$ ratio. Critical Values come from the $[MH]^+$ and $[DAG]^+$, all having their maximum values (100%). The Critical Values represent the smallest value $[MH]^+/\sum[DAG]^+$ could mathematically have and still produce an $[MH]^+$ base peak

fragment ratios are not used to assign the identities of A and B, but their positions.

Jakab et al. [30] demonstrated that the precise percentage composition of regioisomers (LOL and LLO/OLL) could be determined by constructing calibration curves from mixtures of TAG regioisomers with known compositions. Byrdwell [21, 28] tabulated literature $[AA]^+/[AB]^+$ ratios and showed that the percentage compositions of the regioisomers can be calculated from two-point calibration curves based only on the endpoints of the calibration curves reported by Jakab et al. [30], which represented the pure ABA and AAB/BAA regioisomers, as follows:

$$\%ABA = \left(\frac{\left(\frac{[AA]^+}{[AB]^+} \right)_{AAB} - \left(\frac{[AA]^+}{[AB]^+} \right)_{Obs}}{\left(\frac{[AA]^+}{[AB]^+} \right)_{AAB} - \left(\frac{[AA]^+}{[AB]^+} \right)_{ABA}} \right) \times 100 \quad (2)$$

where the subscripts indicate the AAB and the ABA pure regioisomers and Obs indicates the observed $[AA]^+/[AB]^+$ ratio, such as those given in Table 1.

Since few tabulated data for regioisomers are available, Holcapek reported in 2010 the most thorough and useful tabulation of ratios from regioisomers published to date [29]. By transesterification of 11 different three TAG mixtures (e.g.,

PPP+OOO+LLL), mixtures of Type I, Type II, and Type III TAGs were synthesized. The abundances tabulated therein are easily copied and pasted into a spreadsheet and converted to the pure $[AA]^+/[AB]^+$ ratios.

Table 3 shows the results of the application of Eq. 2 with the tabulated values of Holcapek et al. [29] converted to pure ratios and applied to our data in Table 1. The ABA percentage estimations for very long-chain fatty acyl chain (VLCFA)-containing TAGs in Table 3 were based on calibration curves constructed from TAGs containing the longest FA shown [29], arachidic acid, whereas estimations of myristic-acyl chain-containing TAGs were based on corresponding TAGs containing palmitic acid. The TAGs used for these approximations are listed as subscripts next to the names of the TAGs for which no standard appeared in the tabulated data. In all cases, the ratios were sufficiently large or small that these approximations caused no uncertainty in the identification of the predominant regioisomers. Definitive assignments could not be made for "Ca" and "Cy" containing TAGs due to a lack of data for fully saturated or short-chain TAG regioisomer standards. Since values for "ABA" TAGs having few sites of unsaturation were typically in the range 0.2–0.35 (e.g., SOS, OSO, OPO, and OPO) [29], the short-chain TAGs are listed as being in the AAB/BAA forms because of their higher values for Critical Ratio 2. Our instrument has an APCI source very similar to that used on the ThermoScientific Orbitrap XL used by Holcapek et al., so we used data from that instrument for comparison.

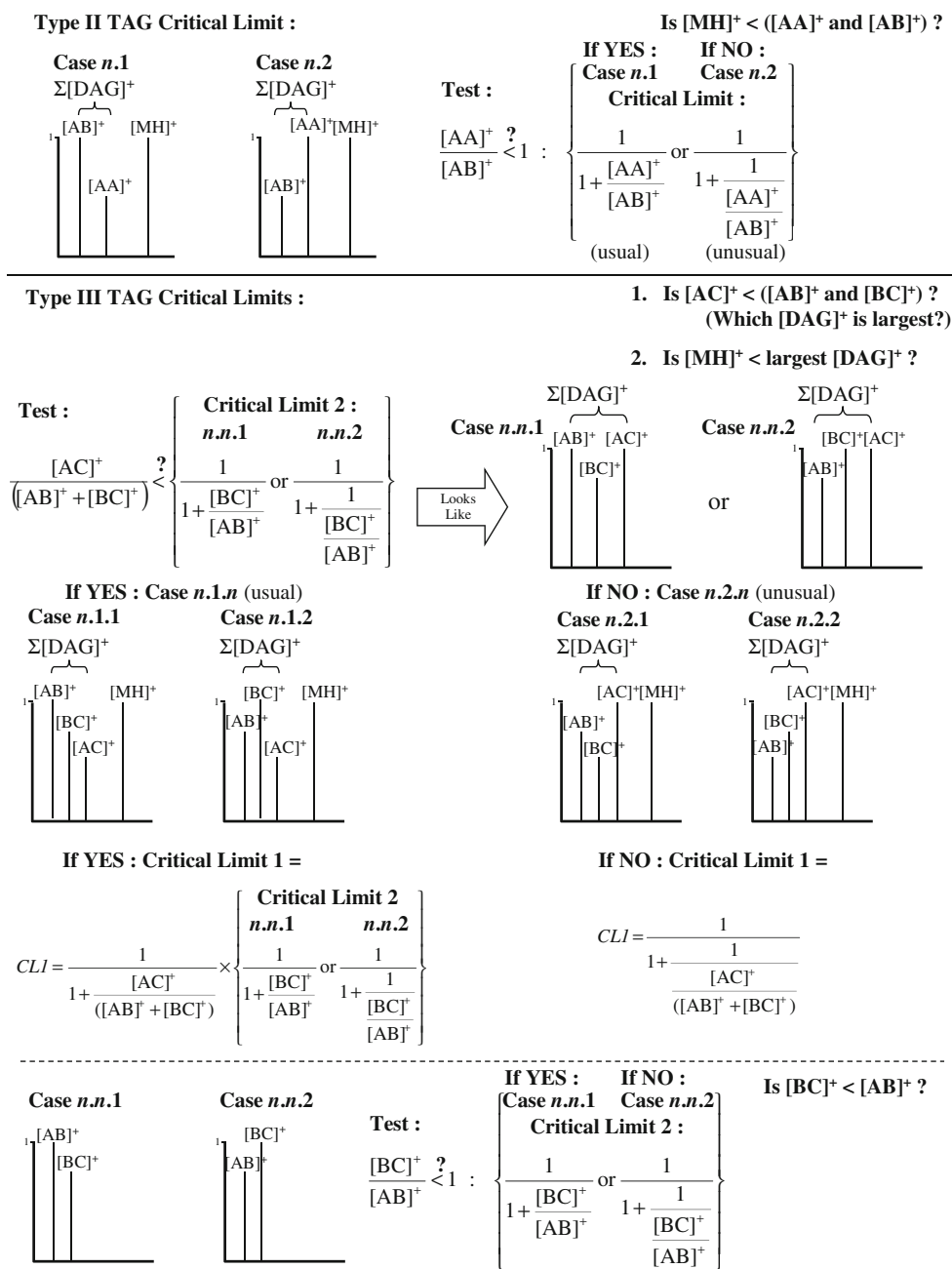
Values of Critical Ratio 2 less than the tabulated value for the ABA regioisomer allowed us to identify the TAG as exclusively the ABA regioisomer, while values greater than the tabulated values (especially when >1) indicated exclusively the "AAB/BAA" regioisomers (0% ABA in Table 3).

Figure 4 shows the shape of the UBUS for a Type II TAG. The $[MH]^+/\sum[DAG]^+$ is plotted as the vertical axis, with the Critical Value of 0.5 and value of 1 shown as red rings at the center and top, respectively, on the vertical axis. The Critical Limit that determines Case 1.n or 2.n is shown as the orange ring between the Critical Value and 1. The second Critical Ratio, $[AA]^+/[AB]^+$, is plotted on the equatorial axis, with the $[AA]^+/[AB]^+$ ratios of pure regioisomers shown plotted going from the lower (dark blue) value for the ABA regioisomer to the higher (lighter blue) value for the AAB/BAA isomers.

Critical Ratio 2 for Type III TAGs: $[AC]^+/([AB]^+ + [BC]^+)$

All TAG names in Table 1 reflect structural assignments based on the fact that loss of the FA in the *sn*-2 position is energetically disfavored, causing the $[sn-1,3AC]^+ [DAG]^+$ to have the lowest abundance of the three $[DAG]^+$ formed from Type III TAGs. This relationship represents the next important aspect of the Interpretation Matrix. The tabulated results of Holcapek

Fig. 3 Generalized representations of mass spectra and equations used to calculate Critical Limits for Type II and Type III TAGs



et al. [29] reflect this trend without exception. In Table 1, a few TAGs have superscripts by them, which indicates that the specification of the $[sn-1,3AC]^+$ regioisomer changed after compensation for the A+2 isotopic abundance. Holcapek et al. described the importance of making this correction. We used calculation based on the Yamamoto approach [37], used by the ChemCalc.org website [38], which gave the same values as Agilent MassHunter software.

The data for Type III TAGs in the report by Holcapek et al. were provided as the three raw abundances for each of the three $[\text{DAG}]^+$ fragments on each instrument. Those data were copied and pasted into a spreadsheet and converted into two

Critical Ratios, Critical Ratio 2, and Critical Ratio 3, provided as ESM Table S1.

Critical Ratio 3 for Type III TAGs: $[\text{BC}]^+ / [\text{AB}]^+$

No distinct trends have been reported for $[sn-1,2\text{DAG}]^+$ fragments versus $[sn-2,3\text{DAG}]^+$ fragments in previous work on APCI-MS of TAGs. It is generally regarded that $sn-1,2$ regioisomers cannot be distinguished from $sn-2,3$ regioisomers by APCI-MS. Therefore, the fragments $[\text{AB}]^+$ and $[\text{BC}]^+$ are not regioispecific in contrast to the $[sn-1,3AC]^+$ fragment discussed above. In all cases discussed here, the

Table 3 Percentage of “ABA” regioisomers of Type II TAGs based on calibration curves from literature values by APCI-MS [29] and observed Critical Ratio 2, $[AA]^+/[AB]^+$, ratios in Table 1

TAG	APCI-MS (%)
LnLLn	90.5
LLnL	70.5
LnOLn	60.7
LnLnP	0 ^a
LLM	0 ^a
LLO	3.2
OLnO	68.1
LLP	0^a
LLG _{LLO}	0 ^a
PLnP	100
OLO	100
MOM _{POP}	100
OOP _{OOA}	0 ^a
LLS	0 ^a
OOM _{OOA}	12.4
PLP	100
LLA	0 ^a
OOP	0
LL-21:0 _{LLA}	0 ^a
OOG _{OOA}	0 ^a
POP	100
LLB _{LLA}	0 ^a
LL-23:0 _{LLA}	0 ^a
OOS	23.1
SLS	60.8
OOE _{OOA}	0 ^a
LLL _{gLLA}	0
LL-25:0 _{LLA}	0 ^a
OOA	7.6
PPS _{PPO}	15.4
LLC _{eLLA}	0 ^a
OO-21:0 _{OOA}	0 ^a
SOS	100
OOB _{OOA}	19.4
OO-23:0 _{OOA}	0
OOL _{gOOA}	23.5
OO-25:0 _{OOA}	0
OOC _{eOOA}	10.5
OOM _{OOA}	0 ^a

Bold value indicates especially clean spectrum. *Italics* indicate interfering peak possible. Subscript_{TAG} indicates no standard Critical Ratio 2 available, substitute TAG standards data used
^a Critical Ratio 2 greater than 1

trend for Critical Ratio 2 is stronger and supersedes the more subtle trends for Critical Ratio 3. In Table 1, we followed the convention mentioned by Byrdwell [28] of setting the $[BC]^+$ fragment equal to the smaller of the two possible abundances for $[AB]^+$ and $[BC]^+$ based on the hypothesis that it may indicate structural trends.

In all cases for Type III TAGs in the APCI-MS data in Table 1, when two polyunsaturated FA were adjacent to each other and were combined with monounsaturated or saturated FAs, the more unsaturated $[DAG]^+$ ended up as the $[AB]^+$

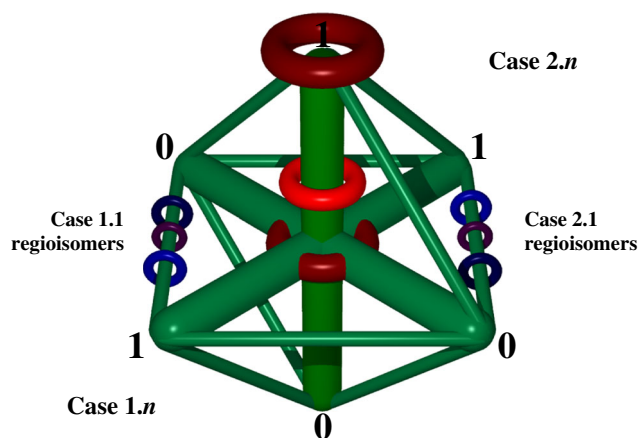


Fig. 4 Shape of the Updated Bottom Up Solution for Type II TAGs. Two Critical Ratios are plotted on axes: vertical axis Critical Ratio 1: $[MH]^+/\Sigma[DAG]^+$, and horizontal axis Critical Ratio 2 $[AA]^+/[AB]^+$. Critical Value for CR1 shown as red ring at 0.5 and value of 1 shown as red ring on top. Critical Limit for CR1 determines Case 1 or Case 2 is orange ring on vertical axis. $[AA]^+/[AB]^+$ can be compared to regioisomer standards, with lower $[AA]^+/[AB]^+$ for ABA TAG shown as dark blue ring, higher $[AA]^+/[AB]^+$ for AAB/BAA TAGs shown as lighter blue ring. Observed $[AA]^+/[AB]^+$ is shown as purple ring

fragments. Type III TAGs containing “LLn/LnL” in Table 1 (LnLM, LLnO, LnLP, LLnA, LLnB, and LnLLg) exemplify this trend. In every case of Type III TAGs, LLn/LnL gave the larger fragment labeled by our convention as $[AB]^+$. Thus, this and the previous data [28] show the same general trend based on Critical Limit 3, which is that the $[DAG]^+$ having more unsaturation tended to form the larger $[AB]^+$ fragments, giving the lower $[BC]^+/[AB]^+$ ratios. However, this trend is not completely simple and straightforward.

Interesting complications to this trend can be seen when the data of Holcapek et al. [29] are converted to Critical Ratios 2 and 3 based on the convention of Byrdwell [28]. Holcapek used a different convention in listing the TAG names and raw abundances, listing the FAs in order of higher to lower mass, such as “OLP” versus “PLO.” When Critical Ratio 3 was constructed so that it was <1 and the TAG names were reversed accordingly, i.e., “OLA” instead of “ALO” (rearranged names in parentheses in ESM Table S1), trends became apparent. As with the data from soybean oil mentioned above, every example of LLn/LnL appearing adjacent as $[AB]^+$ fragments gave Critical Ratio 3 less than 1, i.e., LLnA, LnLA, LLnP, LnLP, LLnO, and LnLO. This indicates that the LLn/LnL $[DAG]^+$ fragment was more stable than the other $[DAG]^+$ fragment, so it remained intact to a higher degree and formed the larger $[DAG]^+$ fragment. Interestingly, in all three corresponding cases when LLn/LnL appeared separated as the $[sn-1,3AC]^+$ regioisomer (LALn, LPLn, and LOLn), the $[DAG]^+$ fragment formed by loss of the polyunsaturated “Ln” FA gave the larger peak, and so it was assigned as $[AB]^+$. To summarize this trend, when “L” and “Ln” were located next to each other, they formed a more stable $[DAG]^+$

fragment, giving a higher abundance, leading it to be assigned as $[AB]^+$ to give a Critical Ratio 3 less than 1, but when the L and Ln were separated from each other by a saturated or monounsaturated FA, the predominant factor became the stability of Ln as a leaving group, causing the remaining $[DAG]^+$ to have the higher abundance, be assigned as $[AB]^+$, and give Critical Ratio 3 < 1. This trend held true for both soybean oil TAGs (Table 1) and regioisomeric standards (ESM Table S1) without exception.

The exactly analogous trend applies to TAGs containing the “OL/LO” $[DAG]^+$. In every soybean oil TAG in Table 1 that contained OL/LO (OLPo, LOM, OLP, OLG, LOS, OLE, OLA, OLB, OLLg, and OLCe) and every regioisomer standard TAG in ESM Table S1 that contained OL/LO adjacent (OLA, LOA, OLS, LOS, OLP, and LOP), the OL/LO $[DAG]^+$ fragment ended up being larger; therefore, it is assigned to $[AB]^+$ to give Critical Ratio 3 < 1 without exception, unless superseded by the trend above (i.e., OLLn and LOLn). Just like the trend above, when the “L” and “O” FAs were *not* next to each other (OAL, OSL, and OPL in ESM Table S1), then *loss* of the polyunsaturated FA L became the predominant mechanism. Thus, if O and L were adjacent, they stabilized each other and formed the most stable (abundant) $[DAG]^+$ fragment, but if they were separated, L formed the most stable leaving group and the $[DAG]^+$ that remained was most abundant. The above trends explain the fragmentation behavior of 18 of the 27 type III TAGs listed in ESM Table S1, which contained LLn/LnL or OL/LO groups.

The remaining nine TAGs in ESM Table S1 contain O and Ln combined with a saturated FA and exhibit a different, but related trend. Six of the nine remaining TAGs had Ln in the *sn*-1 or 3 positions, while three had Ln in the *sn*-2 position. Of those six, five (AOLn, SOLn, OSLn, POLn, and OPLn) obeyed the trend that *loss* of the Ln as a more stable leaving group predominated, giving larger abundances of the $[DAG]^+$ left behind, assigned as $[AB]^+$ by our convention. The one exception was LnAO. In the three TAGs in which Ln was in the *sn*-2 position, two of the three cases (when the saturated FA had a mismatched acyl carbon number (ACN, or chain length), i.e., not=18), i.e., OLnA and OLnP, the $[DAG]^+$ having more unsaturation, $[OLn]^+$, was larger, so it was assigned as $[AB]^+$. However, when the saturated FA was ACN=18, i.e., ‘S’, the $[SLn]^+$ fragment was larger than the $[OLn]^+$ fragment, and so $[OLn]^+/[SLn]^+$ was assigned as Critical Ratio 3 < 1. In summary, seven of nine of the Type III TAGs containing OLn/LnO obeyed the trends mentioned above.

In soybean oil, LnOM did not obey the above trend because it was adversely affected by overlap with LnPPo, in which $[PPo]^+$ was isobaric with $[OM]^+$. Similarly, SLnO was adversely affected by overlap with the much larger OLP peak, with $[OL]^+$ isobaric with $[SLn]^+$, causing anomalous values of Critical Ratios 2 and 3. The peak for soybean oil OLnP was larger than closely surrounding peaks, so it was

assigned with more confidence as the same OLnP as the pure regioisomer.

With all of the trends mentioned above taken together, the fragmentation trends in 25 of 27 regioisomeric standards in ESM Table S1 and the vast majority of Type III TAGs in soybean oil can be characterized by using Critical Ratio 3 constructed according to the convention previously reported by Byrdwell [28], providing new and useful contributions to the Interpretation Matrix for Type III TAGs.

Implementation of the UBUS

The masses of the $[MH]^+$ (or $[MNH_4]^+$ for ESI-MS) and $[DAG]^+$ fragments are dictated by the TAG names in the tables, and the masses are tabulated online at sites found by a search of “LC-MS of triacylglycerols” (including quotes).

Implementation of the UBUS starts the same way as the BUS by calculation of the Critical Limits to allow classification of the Critical Ratios into Cases. The equations below for calculation of the Critical Limits reflect the use of pure ratios instead of percentage ratios. Thus, the equations below are the same as those previously given, except “100” is replaced with “1.” Also, for more clarity, the specific spreadsheet cell addresses provided previously that referred to the positions of the Critical Ratios in the spreadsheet are replaced with abbreviations CR1, CR2_II, CR2_III, and CR3 to refer to Critical Ratios 1, 2, and 3, with the Critical Ratio 2 for Type II and Type III TAGs distinguished, as follows:

Type II:

$$\text{Critical Limit} = \text{IF}(\text{CR2_II} < 1, (1/(1 + \text{CR2_II})), (1/(1 + (1/\text{CR2_II}))))$$

Type III:

$$\text{Critical Limit 2 : CL2} = \text{IF}(\text{CR3} < 1, (1/(1 + \text{CR3})), (1/(1 + (1/\text{CR3}))))$$

$$\text{Critical Limit 1} = \text{IF}(\text{CR2_III} < \text{CL2}, (1/(1 + \text{CR2_III}) * \text{CL2}), (1/(1 + (1/\text{CL2_III}))))$$

These equations (from the “=” to the end of each line) can be copied and pasted in to a spreadsheet next to columns containing the Critical Ratios, and the text “CR2_II,” “CR2_III,” “CR3,” and “CL2” should be replaced with the cell addresses for Critical Ratios 2 and 3 and Critical Limit 2, respectively. Then, these can be pasted down the columns to calculate the Critical Limits. These spreadsheet equations

represent the logic tests “if $CR < CL$, then $1/(1+Ratio)$, else $1/(1+1/Ratio)$ ” described in “Critical Limits” based on the logic pairs shown in Fig. 3, where $CL=1$ for $CR2_II$ and $CR3$. The Excel workbook that allows all of the calculations needed to implement the UBUS is provided in [ESM](#).

In the BUS, the spreadsheet equations for classification into Cases were not explicitly provided. For the UBUS, they are given below and are based on the same logic tests used in the BUS pictured in Schemes [I](#), [II](#), [IIIA](#), and [IIIB](#) and summarized as follows: Type I: “if $CR1 < 1$, Case 1, else Case 2”; Type II: “if $CR1 < CL$, then Case 1.*n*, else Case 2.*n*” and “if $CR2_II < 1$, then Case *n*.1, else Case *n*.2”; and Type III: “if

$CR1 < CL1$, then Case 1.*n.n*, else Case 2.*n.n*” and “if $CR2_III < CL2$, then Case *n*.1.*n*, else Case *n*.2.*n*” and “if $CR3 < 1$, then Case *n.n*.1, else Case *n.n*.2.”

To implement those logic tests, it is helpful to first classify the TAGs as Type I, II, or III. Since the Type corresponds to the number of Critical Ratios, the Type can be determined simply using the =Count() function in Excel applied to the three columns of Critical Ratios, for example =COUNT(CR1:CR3), where CR1 and CR3 are replaced with the first and last columns containing Critical Ratios. If the Type is put in a column labelled “Type,” the equations for Case classification based on the logic tests above are as follows:

To classify Critical Ratio 1:

$$= \text{IF}(\text{Type} = 1, (\text{IF}(CR1 < 1, (1), (2))), (\text{IF}(\text{Type} = 2, (\text{IF}(CR1 < CL, (1), (2))), (\text{IF}(\text{Type} = 3, \text{IF}(CR1 < CL1, (1), (2)), (“-”))))))$$

To classify Critical Ratio 2:

$$= \text{IF}(\text{Type} = 1, (0), (\text{IF}(\text{Type} = 2, (\text{IF}(CR2_II < 1, (1), (2))), (\text{IF}(\text{Type} = 3, \text{IF}(CR2_III < CL2, (1), (2)), (“-”))))))$$

To classify Critical Ratio 3:

$$= \text{IF}(\text{Type} = 1, (0), (\text{IF}(\text{Type} = 2, (0), (\text{IF}(\text{Type} = 3, \text{IF}(CR3 < 1, (1), (2)), (“-”))))))$$

These tests all return “1” for Case 1, “2” for Case 2, “0” for Cases that do not apply to TAGs (i.e., Case *n.n* and *n.n.n* for Type I, and Case *n.n.n* for Type II), and “-” to show an error if the Type is missing.

Alternatively, the Critical Limit equations above can be “nested” into the Case determination equations above to give Case classification without explicitly listing the Critical Limits (as in Table 3 of the BUS [28]). The nested equations are given in the [ESM](#) workbook.

Based on the equations above, the Case classification, shown in the right column of Table 1, is obtained. From these alone, the general form of the mass spectra can be deduced. The exact abundances of the $[MH]^+$ and $[DAG]^+$ for every TAG in the tables are reproduced using the following equations, which were provided as Table 4 in the BUS and now updated in Table 4. The spreadsheet equations have been slightly modified to reflect the simplifications mentioned above, which are the use of pure ratios (the “100”s shown earlier are now “1”s), and the simplification of the Cases to be simply different versions of Case 1 and Case 2. Other small simplifications were made by eliminating extra sets of

optional parentheses that may make the equations more readable, but do not change their meaning or calculated values. One transcription error was found in the previous Table 4 value for $[AB]^+$ for Type II TAGs, which is that the first G7 should have been $1/G7$. This was correctly shown in case 1.4 Scheme I Part II (now Scheme II Case 1.2) and in the spreadsheet results shown in previous Table 5, but was incorrectly transcribed in Table 4 [28]. This has been corrected and updated; Table 4 shows $1/CR2$ for that $[AB]^+$.

In all cases, we calculated the Critical Ratios from the reproduced mass spectrum to ensure that they were identical to the original Critical Ratios. The ability to go back and forth between the Critical Ratios and the mass spectra at will represents an important check of all equations. Table 5 demonstrates the implementation of the UBUS to reproduce the mass spectra of every TAG in Table 1 from the Critical Ratios.

Vitamin D₃

The soybean oil-containing dietary supplement gencaps used as samples for this analysis were labeled to contain 2000 IU

Table 4 Spreadsheet formulas for the implementation of the Updated Bottom Up Solution (UBUS)^a

Type I :

$$[\text{MH}]^+ : =\text{IF}(\text{Casen}=1, (\text{CR1} * 100), 100)$$

$$[\text{AA}]^+ : =\text{IF}(\text{Casen}=1, 100, (1/\text{CR1} * 100))$$

Type II :

$$[\text{MH}]^+ : =\text{IF}(\text{Casen}=1, \text{IF}(\text{Casen.n}=1, (\text{CR1} * (1 + \text{CR2}) * 100), (\text{CR1} * (1 + (1/\text{CR2})) * 100)), 100)$$

$$[\text{AA}]^+ : =\text{IF}(\text{Casen}=1, \text{IF}(\text{Casen.n}=1, \text{CR2} * 100, 100), (1/(\text{CR1} * (1 + (1/\text{CR2})))) * 100)$$

$$[\text{AB}]^+ : =\text{IF}(\text{Casen}=1, \text{IF}(\text{Casen.n}=1, 100, 1/\text{CR2} * 100), (1/(\text{CR1} * (1 + \text{CR2}))) * 100)$$

Type III :

$$[\text{MH}]^+ : =\text{IF}(\text{Casen}=1, \text{IF}(\text{Casen.n}=1, \text{IF}(\text{Casen.n.n}=1, (\text{CR1} * (1 + \text{CR2}) * (1 + \text{CR3}) * 100), (\text{CR1} * (1 + \text{CR2}) * (1 + (1/\text{CR3})) * 100)), (\text{CR1} * (1 + (1/\text{CR2})) * 100)), 100)$$

$$[\text{AC}]^+ : =\text{IF}(\text{Casen}=1, \text{IF}(\text{Casen.n}=1, \text{IF}(\text{Casen.n.n}=1, (\text{CR2} * (1 + \text{CR3}) * 100), (\text{CR2} * (1 + (1/\text{CR3})) * 100)), 100), (1/(\text{CR1} * (1 + (1/\text{CR2}))) * 100))$$

$$[\text{AB}]^+ : =\text{IF}(\text{Casen}=1, \text{IF}(\text{Casen.n}=1, \text{IF}(\text{Casen.n.n}=1, 100, (100 * 1/\text{CR3})), (1/(\text{CR2} * (1 + \text{CR3})) * 100)), (1/(\text{CR1} * (1 + \text{CR2}) * (1 + \text{CR3})) * 100))$$

$$[\text{BC}]^+ : =\text{IF}(\text{Casen}=1, \text{IF}(\text{Casen.n}=1, \text{IF}(\text{Casen.n.n}=1, (\text{CR3} * 100), 100), (1/(\text{CR2} * (1 + (1/\text{CR3}))) * 100)), (1/(\text{CR1} * (1 + \text{CR2}) * (1 + 1/\text{CR3})) * 100))$$

Casen=Case for Critical Ratio 1, CR1; Casen.n=Case for Critical Ratio 2, CR2; Casen.n.n=Case for Critical Ratio 3, CR3

vitamin D₃. Samples were received on January 19, 2010, and the first analyses were conducted on April 20, 2010. The gelpcaps showed an average value of 2011±22 for three analyses conducted in April 2010 and May 2010 or 0.5 % over the label value. The expiration date on the bottle was November 2012. Four analyses conducted in August 2012 gave an average content of 1689±33 or 15.6 % below the label value. Analyses at intermediate dates indicated a steady decline over the 2-year storage time. Samples were stored in a normal refrigerator to replicate the consumer experience.

The most recent values obtained by LC-APCI-MS internal standard (IS) and response factor (RF) approaches were 1759 ±74 for IS and 1722±71 for RF by SIM, 1716±8 and 1732±8 by MRM1 IS and RF, respectively, and 1716±27 and 1743±28 for IS and RF methods by MRM2. The MS values were <100 IU higher than values by UV detection or ~2.5 to 5 % higher by MS than by UV detection.

The APCI-MS mass spectra of vitamin D₂ and vitamin D₃ are simple, giving only two abundances, the [MH]⁺ and [MH-H₂O]⁺. Therefore, a Critical Ratio could be defined for vitamins D₂ and D₃, which is the [MH]⁺/[MH-H₂O]⁺, which has an average value of 1.5458 for vitamin D₃ and 1.5571 for vitamin D₂ by APCI-MS. Since [MH]⁺/[MH-H₂O]⁺ is analogous to [MH]⁺/Σ[DAG]⁺ with only one [DAG]⁺, they can both be treated using Scheme I to give [MH]⁺ and [MH-H₂O]⁺ abundances of 100 and 65 % for vitamin D₃ and 100 and 64 % for vitamin D₂. This demonstrates that the UBUS applies equally well to the two ions for vitamin D as it does to the two ions from a Type I TAG.

Diacylglycerols

DAGs appeared as two peaks representing different regioisomers, which were present at 0.90±0.06 % DAG/

TAG by APCI-MS. Because of this low level, the DAGs are not discussed in detail here, although the percentage compositions and UBUS calculations appear in spreadsheets in the *ESM*. The APCI-MS mass spectra of DAGs are simple, with only two ions: [MH]⁺ and [DAG]⁺ (= [MH-H₂O]⁺); therefore, they can be treated using the same UBUS solution as Type I TAGs. For example, three of the largest peak pairs of DAGs by APCI-MS were: LLn1 (14.2±1.4 % of DAGs) with [MH]⁺/[DAG]⁺=1.6610, LL1 (17.0±2.6 %) with [MH]⁺/[DAG]⁺=0.8176, and OL1 (10.1±0.9 %) with [MH]⁺/[DAG]⁺=0.0810. When these Critical Ratios are processed through the UBUS Scheme I, the following mass spectra are obtained, [MH]⁺ : [DAG]⁺: LLn1: 100 % : 60 %; LL1: 82 % : 100 %; OL1: 8 % : 100 %, which is one Case 1 DAG and two Case 2 DAGs. These values are provided to prove that the UBUS applies equally well to the simple mass spectra of DAGs as it does to TAGs. The degree of unsaturation dictated the fragments ratios of DAGs, similar to TAGs.

Discussion

Conversion of the raw abundances to Critical Ratios has two important benefits. First, it takes fewer values, in the form of Critical Ratios, to express the information contained in a TAG mass spectrum than raw abundances. For Type I TAGs, the [MH]⁺ and [DAG]⁺ fragment can both be reproduced from the single value of Critical Ratio 1, [MH]⁺/Σ[DAG]⁺. For Type II TAGs, the [MH]⁺, [AA]⁺, and [AB]⁺ fragments can all be reproduced from just the two Critical Ratios, [MH]⁺/Σ[DAG]⁺ and [AA]⁺/[AB]⁺. Likewise, the [MH]⁺, [AC]⁺, [AB]⁺, and [BC]⁺ fragments can all be reproduced from just the three Critical Ratios, [MH]⁺/Σ[DAG]⁺, [AC]⁺/([AB]⁺+)

Table 5 Mass spectra abundances calculated from Critical Ratios given in Table 1 processed through the Updated Bottom Up Solution using equations given in Table 4

	[MH] ⁺	[AA] ⁺ or [AC] ⁺	[AB] ⁺	[BC] ⁺
CyCyCy	2	100		
CyCyCa	2	49	100	
CaCaCy	2	56	100	
LnLnLn	100	22		
LnLLn	100	7	15	
LLnL	100	8	17	
LnOLn	100	7	12	
LnLM	100	8	40	13
LnLnP	100	18	13	
LLL	100	38		
LLnO	100	12	16	13
LLM	100	39	25	
LnLP	100	9	23	13
LnPPo	100	25	87	36
LnOM	100	14	42	35
LLO	100	34	39	
OLPo	83	30	100	51
OLnO	100	20	46	
LLP	100	45	34	
LOM	100	42	95	64
PoLP	31	20	100	30
OLnP	100	24	44	24
LLG	100	48	25	
PLM	10	65	100	95
PLnP	43	29	100	
OLO	84	26	100	
MOM	10	27	100	
OOPo	9	100	18	
LLS	100	38	34	
LLnA	100	14	26	22
OLP	66	51	100	50
SlnO	18	6	100	8
OOM	32	47	100	
PoPO	31	68	100	72
OLG	100	15	100	65
PLP	5	38	100	
POM	14	48	100	93
OOO	24	100		
LLnB	100	16	20	16
LLA	100	38	31	
LGP	100	26	46	27
LOS	69	47	100	50
OOP	20	60	100	
LL21:0	100	51	30	
OLE	100	38	77	53
SLP	8	70	100	86
OOG	27	100	64	

Table 5 (continued)

	[MH] ⁺	[AA] ⁺ or [AC] ⁺	[AB] ⁺	[BC] ⁺
LnLLg	100	14	21	16
POP	7	27	100	
LLB	100	35	31	
OLA	79	61	100	74
PGO	45	62	100	71
LL23:0	100	36	28	
OOS	19	51	100	
OL21:0	54	37	100	37
PPP	0	100		
PAL	12	36	100	53
SLS	6	51	100	
OOE	13	100	27	
LLLg	100	32	34	
SOP	13	26	100	88
OLB	81	65	100	70
EPO	57	81	100	84
GSO	56	44	100	52
LL25:0	100	41	31	
OOA	23	51	100	
LO23:0	68	51	100	54
LBP	11	66	100	97
SAL	11	48	100	54
PPS	0	66	100	
LLCe	100	38	31	
OO21:0	22	100	98	
AOP	42	83	100	84
SOS	10	20	100	
OLLg	82	71	100	80
OOB	22	47	100	
LO25:0	59	44	100	45
PLgL	11	42	100	58
SBL	11	59	100	85
OO23	19	72	100	
BOP	18	74	100	78
OLCe	72	52	100	66
SAO	24	55	100	65
OOLg	19	46	100	
SLgL	11	91	100	98
OO25	18	91	100	
OLgP	17	73	100	72
BOS	16	65	100	80
OOCe	21	50	100	
LSCe	8	64	100	77
LgOS	16	83	100	70
OOMo	21	100	51	

[BC]⁺), and [BC]⁺/[AB]⁺. For this reason, the Critical Ratios constitute a “reduced” or “compact” data set where all the

information is expressed in fewer values. Second, the Critical Ratios actually provide *more information* in those *fewer values*. For instance, by using Critical Ratio 3 for analysis of the data in Table 3 of Holcapek et al. [29], we were able to identify trends that have not been reported before. Similarly, we were able to use Critical Ratio 1 in Fig. 1 to show a new model that provides a good approximation of average ratios of $[MH]^+/\Sigma[DAG]^+$ for TAGs based only on the degree of unsaturation. Likewise, Critical Ratio 2 can be entered directly at face value into Eq. 2 above (Eq. 3 in [28]) to estimate or quantify the percentages of regioisomers.

Based on these principles, if the two values for each TAG in Table 2 by Holcapek et al. [29] were replaced by the two values of Critical Ratio 1 and Critical Ratio 2, not only would the same information have been conveyed regarding regioisomers but also that table would have become a library of mass spectra of Type II TAGs, by which the $[MH]^+$, $[AA]^+$, and $[AB]^+$ fragments for every TAG in the table could be reproduced. Similarly, if the three values (normalized abundances) in Table 3 by Holcapek et al. [29] were replaced by the three values of Critical Ratios 1, 2, and 3, then not only would all of the information discussed in that report have been equally valid but also the trends presented in this report would have been visible, providing additional information, and furthermore, that table would have become a library of mass spectra of Type III TAGs since the $[MH]^+$, $[AC]^+$, $[AB]^+$, and $[BC]^+$ abundances for every TAG in the table could be reproduced by processing the Critical Ratios through the UBUS given here (or the BUS given previously).

It should be mentioned that the mass spectra calculated from the BUS and UBUS can be calculated from the Critical Ratios regardless of whether they are <1 or >1 . It is a bounded system that applies to all Critical Ratios from 0 to ∞ . The convention to assign Critical Ratio 3 <1 is part of the Interpretation Matrix, with the intention of deducing structural information from the Critical Ratios.

Space limitation in this report prohibits detailed discussion of the UBUS applied to ESI-MS, ESI-MS/MS, and APPI-MS data. Nevertheless, “quadruple parallel mass spectrometry” data not included here prove that the UBUS applies equally well to mass spectra from any of these API-MS (or MS/MS) techniques. The UBUS can also be used for other classes of molecules, such as diacylglycerols and vitamin D.

Acknowledgments The work of Dr. Robert Goldschmidt in assisting with some integration and reporting functions is gratefully acknowledged. This work was supported by the USDA Agricultural Research Service. Mention or use of specific products or brands do not represent or imply endorsement by the USDA.

Compliance with ethical standards The author declares no potential conflicts of interest with respect to the performance of experiments, authorship, or publication of this article.

References

- Hunter JE (2001) Studies on effects of dietary fatty acids as related to their position on triglycerides. *Lipids* 36(7):655–668
- Schwab U, Lauritzen L, Tholstrup T, Haldorsson T, Riserus U, Uusitupa M, Becker W (2014) Effect of the amount and type of dietary fat on cardiometabolic risk factors and risk of developing type 2 diabetes, cardiovascular diseases, and cancer: a systematic review. *Food Nutri Res* 58. doi:10.3402/fnr.v58.25145
- Bézar J, Blond JP, Bernard A, Clouet P (1994) The metabolism and availability of essential fatty acids in animal and human tissues. *Reprod Nutr Dev* 34(6):539–568
- Mu H, Porsgaard T (2005) The metabolism of structured triacylglycerols. *Prog Lipid Res* 44(6):430–448. doi:10.1016/j.plipres.2005.09.002
- Karupaiah T, Sundram K (2007) Effects of stereospecific positioning of fatty acids in triacylglycerol structures in native and randomized fats: a review of their nutritional implications. *Nutr Metab* 4. doi:10.1186/1743-7075-4-16
- Dubois V, Breton S, Linder M, Fanni J, Parmentier M (2007) Fatty acid profiles of 80 vegetable oils with regard to their nutritional potential. *Eur J Lipid Sci Technol* 109(7):710–732. doi:10.1002/ejlt.200700040
- Byrdwell WC, Emken EA (1995) Analysis of triglycerides using atmospheric pressure chemical ionization mass spectrometry. *Lipids* 30(2):173–175. doi:10.1007/BF02538272
- Neff WE, Byrdwell WC (1995) Soybean oil triacylglycerol analysis by reversed-phase high-performance liquid chromatography coupled with atmospheric pressure chemical ionization mass spectrometry. *JAOCS, J Am Oil Chem Soc* 72(10):1185–1191
- Byrdwell WC, Emken EA, Neff WE, Adlof RO (1996) Quantitative analysis of triglycerides using atmospheric pressure chemical ionization-mass spectrometry. *Lipids* 31(9):919–935
- Laakso P, Voutilainen P (1996) Analysis of triacylglycerols by silver-ion high-performance liquid chromatography-atmospheric pressure chemical ionization mass spectrometry. *Lipids* 31(12):1311–1322
- Laakso P (1997) Characterization of alpha- and gamma-linolenic acid oils by reversed-phase high-performance liquid chromatography-atmospheric pressure chemical ionization mass spectrometry. *JAOCS, J Am Oil Chem Soc* 74(10):1291–1300
- Duffin KL, Henion JD, Shieh JJ (1991) Electrospray and tandem mass spectrometric characterization of acylglycerol mixtures that are dissolved in nonpolar solvents. *Anal Chem* 63(17):1781–1788
- Cheng C, Gross ML, Pittenauer E (1998) Complete structural elucidation of triacylglycerols by tandem sector mass spectrometry. *Anal Chem* 70(20):4417–4426
- Schuyt PJW, De Joode T, Vasconcellos MA, Duchateau GSMJE (1998) Silver-phase high-performance liquid chromatography-electrospray mass spectrometry of triacylglycerols. *J Chromatogr A* 810(1–2):53–61. doi:10.1016/S0021-9673(98)00277-5
- Hsu FF, Turk J (1999) Structural characterization of triacylglycerols as lithiated adducts by electrospray ionization mass spectrometry using low-energy collisionally activated dissociation on a triple stage quadrupole instrument. *J Am Soc Mass Spectrom* 10(7):587–599
- Hvattum E (2001) Analysis of triacylglycerols with non-aqueous reversed-phase liquid chromatography and positive ion electrospray tandem mass spectrometry. *Rapid Commun Mass Spectrom* 15(3):187–190. doi:10.1002/1097-0231(20010215)15:3<187::AID-RCM211>3.0.CO;2-T
- Marzilli LA, Fay LB, Dionisi F, Vouros P (2003) Structural characterization of triacylglycerols using electrospray ionization-MSn ion-trap MS. *JAOCS, J Am Oil Chem Soc* 80(3):195–202
- Byrdwell WC (2001) Atmospheric pressure chemical ionization mass spectrometry for analysis of lipids. *Lipids* 36(4):327–346

19. Mottram HR (2005) Regioisomeric analysis of triacylglycerols using high performance liquid chromatography/ atmospheric pressure chemical ionization mass spectrometry. In: Byrdwell WC (ed) *Modern Methods for Lipid Analysis by Liquid Chromatography/ Mass Spectrometry and Related Techniques*. AOCS Press, Champaign, pp 276–297
20. Řezanka T, Sigler K (2007) The use of atmospheric pressure chemical ionization mass spectrometry with high performance liquid chromatography and other separation techniques for identification of triacylglycerols. *Curr Anal Chem* 3(4):252–271. doi:10.2174/157341107782109644
21. Byrdwell WC (2005) Qualitative and quantitative analysis of triacylglycerols by atmospheric pressure ionization (APCI and ESI) mass spectrometry techniques. In: Byrdwell WC (ed) *Modern methods for lipid analysis by liquid chromatography/ mass spectrometry and related techniques*. AOCS Press, Champaign, pp 298–412
22. Murphy RC, Leiker TJ, Barkley RM (2011) Glycerolipid and cholesterol ester analyses in biological samples by mass spectrometry. *Biochim Biophys Acta Mol Cell Biol Lipids* 1811(11):776–783. doi:10.1016/j.bbalip.2011.06.019
23. Cozzolino R, De Giulio B (2011) Application of ESI and MALDI-TOF MS for triacylglycerols analysis in edible oils. *Eur J Lipid Sci Technol* 113(2):160–167
24. Sandra K, Sandra P (2013) Lipidomics from an analytical perspective. *Curr Opin Chem Biol* 17(5):847–853. doi:10.1016/j.cbpa.2013.06.010
25. Cajka T, Fiehn O (2014) Comprehensive analysis of lipids in biological systems by liquid chromatography-mass spectrometry. *TrAC Trends Anal Chem* 61:192–206. doi:10.1016/j.trac.2014.04.017
26. Mottram HR, Evershed RP (1996) Structure analysis of triacylglycerol positional isomers using atmospheric pressure chemical ionisation mass spectrometry. *Tetrahedron Lett* 37(47):8593–8596
27. Fauconnot L, Hau J, Aeschlimann JM, Fay LB, Dionisi F (2004) Quantitative analysis of triacylglycerol regioisomers in fats and oils using reversed-phase high-performance liquid chromatography and atmospheric pressure chemical ionization mass spectrometry. *Rapid Commun Mass Spectrom* 18(2):218–224
28. Byrdwell WC (2005) The bottom-up solution to the triacylglycerol lipidome using atmospheric pressure chemical ionization mass spectrometry. *Lipids* 40(4):383–417. doi:10.1007/s11745-006-1398-9
29. Holcapek M, Dvorakova H, Lisa M, Giron AJ, Sandra P, Cvacka J (2010) Regioisomeric analysis of triacylglycerols using silver-ion liquid chromatography-atmospheric pressure chemical ionization mass spectrometry: comparison of five different mass analyzers. *J Chromatogr A* 1217(52):8186–8194
30. Jakab A, Jablonkai I, Forgács E (2003) Quantification of the ratio of positional isomer dilinoleoyl-oleoyl glycerols in vegetable oils. *Rapid Commun Mass Spectrom* 17(20):2295–2302
31. Manninen P, Laakso P (1997) Capillary supercritical fluid chromatography-atmospheric pressure chemical ionization mass spectrometry of triacylglycerols in berry oils. *JAOCS, J Am Oil Chem Soc* 74(9):1089–1098
32. Byrdwell WC (2011) “Dilute-and-shoot” triple parallel mass spectrometry method for analysis of vitamin D and triacylglycerols in dietary supplements. *Anal Bioanal Chem* 401(10):3317–3334. doi:10.1007/s00216-011-5406-4
33. Byrdwell WC (2013) Quadruple parallel mass spectrometry for analysis of vitamin D and triacylglycerols in a dietary supplement. *J Chromatogr A* 1320:48–65. doi:10.1016/j.chroma.2013.10.031
34. Byrdwell WC, Neff WE, List GR (2001) Triacylglycerol analysis of potential margarine base stocks by high-performance liquid chromatography with atmospheric pressure chemical ionization mass spectrometry and, flame ionization detection. *J Agric Food Chem* 49(1):446–457. doi:10.1021/jf0008801
35. Byrdwell WC (2014) Extract-filter-shoot liquid chromatography with mass spectrometry for the analysis of vitamin D2 in a powdered supplement capsule and standard reference material 3280. *J Sep Sci* 37(16):2095–2110. doi:10.1002/jssc.201400234
36. Byrdwell WC, Neff WE (1997) Qualitative and quantitative analysis of triacylglycerols using atmospheric pressure chemical ionization mass spectrometry. In: McDonald RE, Mossoba MM (eds) *New techniques and applications in lipid analysis*. AOCS Press, Champaign, pp 45–80
37. Yamamoto H (1977) Calculations of isotopic distribution in molecules extensively labeled with heavy isotopes. *Anal Chem* 49(2):281–283
38. Patiny L, Borel A (2013) ChemCalc: a building block for tomorrow’s chemical infrastructure. *J Chem Inf Model* 53(5):1223–1228. doi:10.1021/ci300563h